The 5th European sCO_2 Conference for Energy Systems
March 14-16, 2023, Prague, Czech Republic

2023-sCO2.eu-139

INFLUENCE OF VARIATIONS OF FLUE GAS AND AMBIENT TEMPERATURE ON THE DYNAMICS AND PERFORMANCE OF A MW SCALE SUPERCRITICAL CO2 WASTE HEAT TO POWER UNIT

Olumide Olumayegun
Brunel University London
Uxbridge, United Kingdom

Matteo Marchionni
Brunel University London
Uxbridge, United Kingdom
Email: matteo.marchionni2@brunel.ac.uk

Muhammad Usman
Brunel University London
Uxbridge, United Kingdom

Savvas A Tassou*
Brunel University London
Uxbridge, United Kingdom

ABSTRACT

Waste heat availability from many industrial plant can vary not only during start up and shut down of the process but also as a response to many other factors such as process control and varying demand of heat by diverse and distinct unit operations in the plant.

Implementing heat recovery from exhaust waste heat for power generation purposes, therefore, requires knowledge of the variation in the mass flow rate and temperature of the waste heat as well as variations in other conditions that affect the performance of the power generation system such as the temperature and flow rate of the heat sink medium.

This paper presents a numerical model and simulation results of the dynamic behaviour of a 2.0 MWe sCO_2 power system, designed to recover heat from the exhaust gases of a cement manufacturing plant. The design employs an indirect heat recovery loop utilising thermal oil as the heat transfer medium and direct heat rejection from the CO_2 gas cooler to the ambient.

The results show that fluctuations in the exhaust gas conditions within the operating range of the sCO_2 power system are damped by the large quantity of heat transfer fluid in the indirect heat transfer loop and do not present a significant challenge to the control of the conditions entering the turbine. On the other hand, the limited thermal mass of the gas cooler does not have the capacity to absorb significant quantities of thermal energy and as a result the response of the sCO_2 system to variations in ambient temperature is much faster than the response to changes in exhaust gas temperature and flow rate. This will require a more sophisticated control strategy to ensure the sCO_2 temperature at inlet to the compressor and other components remains within the design operating range.

INTRODUCTION

The recovery of waste heat from existing industrial facilities is considered among the most promising ways to improve their energy efficiency, create new business opportunities and mitigate their carbon footprint [1]. However, despite intensive research effort and interest in recent years, there are still challenges in the exploitation of industrial waste heat sources. The availability of waste heat, temperature and composition of the heat carrier, the intensity or modality of supply, and the ease or economic feasibility of its re-utilization are critical factors for the selection and design of the waste heat recovery (WHR) technology [2].

For the recovery of high temperature waste heat, over 300°C, bottoming thermodynamic cycles, such as the emerging supercritical carbon dioxide (sCO_2) power systems, offer the potential of high energy conversion efficiency [3]. Carbon dioxide has very good thermo-physical properties. It is a non-toxic, non-flammable and thermally stable compound and in its supercritical state, has properties, including high density, that can lead to high cycle efficiencies and a substantial reduction in the size of components compared to alternative heat to power conversion technologies [3].

Smaller components present lower metal mass and less thermal inertia, making the technology attractive for its higher operational flexibility and fast response to variations in waste heat availability. These advantages have driven academic and industrial research in recent years to investigate sCO_2 power cycles for WHR applications. Many works are available in the literature on thermodynamic design and optimization [4,5], techno-economic analysis [6], system and standalone component modelling [7–11], and system off-design analysis [12,13]. However, less attention has been devoted to the transient dynamics of this cycle and its control, mainly due to the unavailability, as yet, of large pilot plants and experimental facilities for the investigation of fully integrated power cycles.

* corresponding author(s)

DOI: 10.17185/duepublico/77321

Understanding of the dynamic behaviour of sCO_2 waste heat to power systems is very important for WHR applications since waste heat availability from the topping manufacturing process, can vary on hourly, daily and weekly basis due to variations in the manufacturing processes in the plant, including start-up and shut-downs, and ambient temperature. The latter has an indirect influence on thermal energy inputs and heat losses from the manufacturing processes.

Variations in the temperature and flowrate of the exhaust gases will be reflected in variations in the sCO_2 cycle's thermodynamic conditions, i.e. the temperature of CO_2 at the outlet of the primary heat exchanger (where the waste heat recovery occurs) and, therefore, at the turbine inlet. Such variations if are not mitigated by the control of the sCO_2 power system, may impact on the functional integrity of the components and system itself, with detrimental impacts on the long-term performance of the unit and its operational lifetime.

To understand how these effects can be mitigated, the dynamic behaviour of the system during transient operating conditions must be investigated to provide useful insights from a controls perspective.

To fill this gap this research focuses on the transient analysis of a 2.0 MWe sCO_2 power system for the recovery of waste heat from a cement plant. Such system is being developed in the framework of the CO2OLHEAT project, funded by the EU [14].

The sCO2 system employs an indirect heat recovery loop utilising thermal oil as the heat transfer medium and direct heat rejection from the CO2 gas cooler to the ambient. Equation based models have been used for the turbomachines and the heat exchangers (waste heat recovery unit, primary heater, recuperator and gas cooler). In particular, heat exchangers are modelled using a one-dimensional approach whilst turbomachines are considered as lumped objects given their faster dynamics.

For the analysis, real data for the flue gas have been used from a CEMEX cement plant at Prachovice in Czechia. After presenting the modelling methodology, the paper presents results of the transient response of the sCO_2 system to step variations of flue gas temperature and flowrate and variations in ambient temperature during a typical day's operation of the cement plant. The modelling results are very useful for the development of control strategies to ensure stable and efficient operation whilst maintaining the integrity of the major components in the system.

CEMENT PLANT

A schematic diagram of the cement facility at Pracovice is shown in Figure 1. After the rotary kiln (point 1), the exhaust gases pass through the pre-heater (point 2) before entering the conditioning towers (points 5 and 6), to be finally rejected to the environment from the stack (point 7). A position for the possible installation of the heat recovery unit was selected to be before the conditioning tower, between points 3 and 4 in Figure 1, to maximise heat recovery potential.

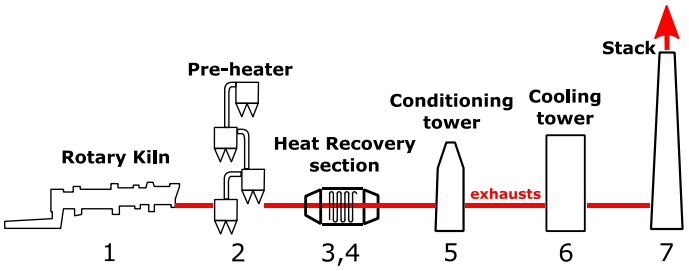

Figure 1: Schematic of the cement plant showing position of measurement of the exhaust flowrate and temperature.

The waste heat recovery units (two units in parallel), use an intermediate heat transfer carrier, thermal oil, to recover heat from the exhaust gases. The oil transfers this heat to the sCO_2 power block through the primary heater, Figure 2. At the outlet of the heater, point 5 in Figure 2, the sCO_2 is at high pressure and temperature, and is expanded in the first turbine unit (T), which drives the compressor unit (C). A helper motor provides additional power when the power from the turbine is not sufficient to drive the compressor, for example at start-up. Both the compressor and the turbine units are two-stage machines.

After the first expansion, the sCO_2 flows into an axial power turbine (PT), which is designed to generate 2.2 MW of power (Figure 2). An air cooler is designed to use ambient air to reject heat from the sCO_2 flow and restore the initial cycle conditions.

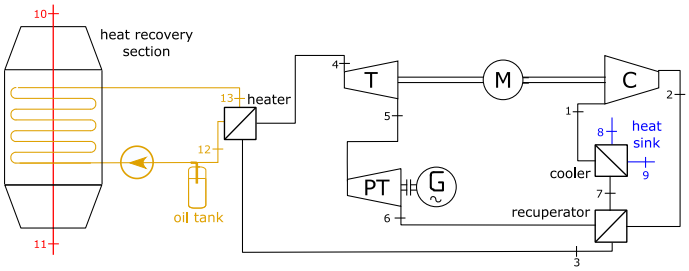

Figure 2: CO2OLHEAT sCO_2 simplified cycle representation.

MODELLING METHODOLOGY

The dynamic model of the sCO_2 WHR plant has been implemented in the MatLab Simulink® programming and simulation environment using sFunctions [15]. Such model can be divided into three main parts: i) the intermediate heat transfer oil loop; ii) the sCO_2 power block and iii) the interface between the power block and the exhaust gases in the WHRU and the power block and the air in the gas cooler. These domains include individual component sub-models such as heat exchangers, pipes, pumps, expansion tank, and turbomachinery.

The models have been developed using mass, energy and momentum conservation equations as well as other constitutive equations. The thermodynamic and physical properties of CO_2 and flue gas have been determined using NIST Refprop (version 10.0) [16] while the properties of the heat transfer oil (FRAGOLTHERM® X-76-A) have been obtained from the oil manufacturer.

DOI: 10.17185/duepublico/77321

The different components have been represented as independent blocks having input and output ports for interconnection between components in accordance with the plant layout. For example, the port carrying information about the fluid flow, contains details on the mass flow rate, pressure and temperature of the fluid stream. This results in a model which provides a more realistic visual representation of the plant. The models of the different system components are presented in the following sections.

Pipe model

The implementation of the mass, energy and momentum conservation equations for fluid flow in pipes as well as in heat exchanger ducts follows the rigorous modelling approach of Franke et al. [17].

The conservation of mass equation for the pipe is given as:

$$A\frac{\partial \rho}{\partial t} + \frac{\partial \dot{m}}{\partial x} = 0 \tag{1}$$

which, for a pipe section of cross-sectional area, A, can be written as a derivative of pressure and specific enthalpy:

$$A(\Delta L)\left[\frac{\partial \rho}{\partial p}\frac{\partial p}{\partial t} + \frac{\partial \rho}{\partial h}\frac{\partial h}{\partial t}\right] + \Delta \dot{m} = 0 \tag{2}$$

The governing equation for the conservation of energy can be written as:

$$A\frac{\partial(\rho u)}{\partial t} + \frac{\partial(\dot{m}h)}{\partial x} - \omega\varphi = 0 \tag{3}$$

$$A(\Delta L)\left[(h\frac{\partial \rho}{\partial p} - 1)\frac{\partial p}{\partial t} + (\rho + h\frac{\partial \rho}{\partial h})\frac{\partial h}{\partial t}\right] + \Delta(\dot{m}h) - Q = 0 \tag{4}$$

For the pipe model, the heat loss, Q, is assumed to be negligible. The momentum conservation equation, ignoring the gravitational force term, can be expressed as:

$$\frac{\partial \dot{m}}{\partial t} + A\frac{\partial p}{\partial x} + A\frac{\partial(\rho v^2)}{\partial x} + f\frac{\dot{m}^2}{2\rho D_h A} = 0 \tag{5}$$

$$\Delta L\frac{\partial \dot{m}}{\partial t} + A(\Delta p) + \frac{\Delta(\dot{m}^2/\rho)}{A} + f\frac{\Delta L}{2D_h A}\frac{\dot{m}^2}{\rho} = 0 \tag{6}$$

Heat exchanger model

The WHRU, PHE and recuperator were modelled as counter-flow heat exchangers. The ACHE was discretised into nodes and modelled as a cross-flow heat exchanger. Figure shows the implementation of the discretised model of the ACHE in Matlab®/Simulink®.

The heat exchanger models consider the hot stream, cold stream and the separating metal wall. The hot and cold stream mass, energy and momentum conservation equations are similar to those used for the pipe model above. The dynamics of the separating metal wall temperature were modelled using the approach outlined in Olumayegun and Wang [22]:

$$M_w C_w \frac{dT_w}{dt} = Q_h - Q_c \tag{7}$$

Where, Q_h and Q_c represent the heat transferred from the hot stream to the metal and from the metal wall to the cold stream respectively.

$$Q_h = U_h A_s (T_h - T_w) \tag{8}$$

$$Q_c = U_c A_s (T_w - T_c) \tag{9}$$

U_h and U_c represent the convective heat transfer coefficients and A_s is the surface area for heat transfer.

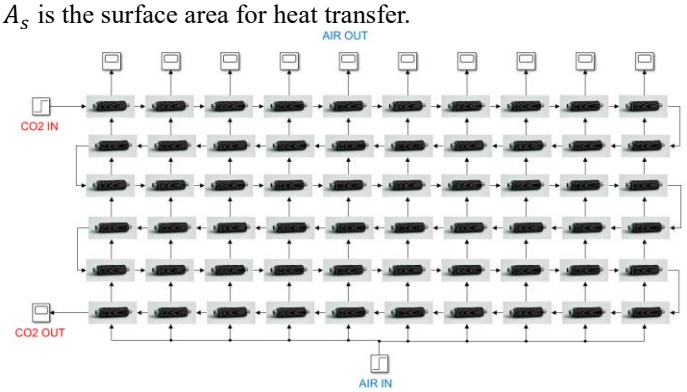

Figure 3: Descritised dynamic modelling of air-cooled heat exchanger (ACHE) in Matlab®/Simulink®.

Compressor and turbine models

The modelling of CO_2 compressors is challenging due to the non-ideal gas properties of CO_2 close to the critical point. One modelling approach presented in the literature considers the use of corrected performance maps taking into account the compressibility of the gas close to the critical conditions [18]. Despite good prediction accuracy away from the critical point, this method has been found to decrease in accuracy at operation close to the CO_2 critical conditions [9, 19]. A more reliable method suggested for compressor modelling by Gong et. al. [20], is the one developed for incompressible turbomachinery (pumps). According to the authors, when the sCO_2 compressor is treated like a pump, its estimated work is within 2% of that computed using real gas CO_2 properties. Thus, instead of correcting the mass flow rate using the method for ideal gas turbomachinery, the flow coefficient of the compressor can be determined from [18- 21]:

$$\phi = \frac{\dot{m}}{U\rho} \tag{10}$$

Where U is the impeller tip speed and ρ is the fluid density. For the turbine, the CO_2 working fluid can be considered as ideal gas and the flow coefficient can be taken as per Equation (11) [20].

DOI: 10.17185/duepublico/77321

$$\phi = \frac{\dot{m}\sqrt{T_{in}}}{p_{in}} \quad (11)$$

The turbomachinery performance map, which gives the pressure ratio and efficiency as function of the flow coefficient is used to determine the pressure ratio and efficiency of the compressor and turbine. The turbomachinery outlet conditions and power are then calculated from the pressure ratio and efficiency. Further details about the turbomachinery modelling approach can be found in Olumayegun and Wang [22].

Integrally geared shaft models

The compressors are driven by an expander supported by an electric motor. The compressors, expander and motor are positioned on separate shafts rotating at different speeds. The compressors and expander shafts are connected to the motor shaft through an integral gear system. The transient of the motor shaft speed, N_m, can be determined from the shaft dynamic equation [22]:

$$\left(I_m + I_{exp} + I_{LPC} + I_{HPC}\right)N_m \frac{dN_m}{dt} = (P_m + P_{exp} - P_{LPC} - P_{HPC} - P_{loss}) \quad (12)$$

Where I represents the inertia and P the power.

The motor-expander and motor-compressor gear ratio are given by Equation (13) and (14).

$$R_{m-exp} = \frac{N_m}{N_{exp}} \quad (13)$$

$$R_{m-cc} = \frac{N_m}{N_{cc}} \quad (14)$$

Oil tank model

The expansion tank is assumed to have a cross-sectional area, A, with a fluid level of height, H. The mass and energy conservation equations for the fluid in the tank can be expressed as:

$$\frac{dM}{dt} = \dot{m}_{in} - \dot{m}_{out} \quad (15)$$

$$\frac{d(Mh)}{dt} = \dot{m}_{in}h_{in} - \dot{m}_{out}h_{out} \quad (16)$$

Where h is the specific enthalpy of heat transfer fluid and M is the mass of fluid in the tank.

$$M = \rho AH \quad (17)$$

The pressure of the oil at the tank outlet is given as:

$$p_{out} = p_{atm} + \rho gH \quad (18)$$

Where ρ is the density of oil and g is acceleration due to gravity.

RESULTS AND DISCUSSIONS

Steady state simulation results at design operating point

In this study, the design operating point values for the sCO_2 plant were based on the operating data of the exhaust gas from the cement plant and ambient air conditions. The main parameters for the model related to the system components have been taken from the preliminary design stage of the CO2OLHEAT demonstrator and are reported in Table 1. The compressor designed by Baker Hughes, which is a partner in the CO2OLHEAT project, considers two compressor stages with isentropic efficiency at nominal conditions of 86% for stage 1 and 80% for stage 2. Design data for the heat exchangers are given in Table 2.

Table 1: Operating conditions and performance of sCO_2 plant at the design point.

Parameters	Value
Compressor	
Isentropic efficiency	86%/80 %
Nominal power	887 kW
Expander	
Isentropic efficiency	81%
Power	783 kW
Power-turbine	
Isentropic efficiency	83%
Power	2355 kW
Heat exchangers thermal duty	
PHE	9128 kW
PCHE	10479 kW
ACHE	6876 kW
WHRU	9114 kW
Intermediate thermal oil loop	
Oil tank volume	36 m^3
Total oil volume	72 m^3

Table 2: Performance and design parameters of sCO_2 plant at the design point.

Heat Exchanger design parameters	WHRU	PHE	PCHE	ACHE
Fluid (hot/cold)	FG/Oil	Oil/CO2	CO2/CO2	CO2/Air
Surface area [m^2]	1328	114	194	16600
Pressure loss (hot/cold side) [kPa]	10/50	50/350	100/100	127/10
Overall heat transfer coefficient [w/m^2K]	351	1020	1912	40
Volume [m^3]	25	2.3	0.3	276
Dry mass [kg]	9800	841	4940	15600

DOI: 10.17185/duepublico/77321

Tables 3 and 4 show the results of the steady-state simulations which are in agreement with the thermodynamic design carried out for the CO2OLHEAT demonstrator. In particular, Table 3 shows the thermodynamic state points of the plant (numbers refer to Figure 2) for the different circuits (sCO_2 power block, cooling air and intermediate thermal oil loop). Table 4, reports the main results from the steady state simulation. It can be seen that the sCO_2 heat recovery plant should be able to recover approximately 9 MWth of waste heat from the exhaust gases and convert it to 2 MWe of electrical power with an efficiency of approximately 22%.

Table 3: Results of steady state simulation

State	$\dot{m}$ (kg/s)	P (bar)	T (^{0}C)	h (kJ/kg)
SCO2 loop				
1	41	85	33	294
2	41	215	58	316
3	41	214	187	575
4	41	210	360	800
5	41	171	339	781
6	41	88	275	723
7	41	87	68	464
Cooling air				
8	298	1	20	419
9	298	1	43	442
10	131	1	400	1048
11	131	1	342	978
Intermediate thermal oil loop				
12	61	14	317	739
13	61	14	386	887

Table 4: Performance parameters of sCO2 plant at the design point.

Parameters	Value
Compressor Rotational speed	19500 RPM
Expander Rotational speed	12500 RPM
Generator power	2205 kW
Generator power	2205 kW
Turboexpander motor power	211 kW
Net power output	1994 kW
Cycle thermal efficiency	22 %

Open loop dynamic response to step change in exhaust gas and ambient air conditions

The main sources of external disturbance for the sCO_2 WHP plant are the fluctuation in the cement plant exhaust gas and ambient conditions. In particular, the exhaust gas temperature and mass flow rate can vary as a result of variations in process operations and their control, while variations in the flow of the air across the gas cooler can result from control actions or failure of heat exchanger fans.

For these reasons, open loop simulation of the sCO_2 plant (i.e. without control actions) have been carried out considering step changes in these variables to provide insights into the inherent transient behaviour of the cycle due to such changes [22]. Open loop transient response results can also inform the choice of potential control variables and strategies. Tables 4, 5 and 6 summarise the main results and assumptions of the three open loop simulations.

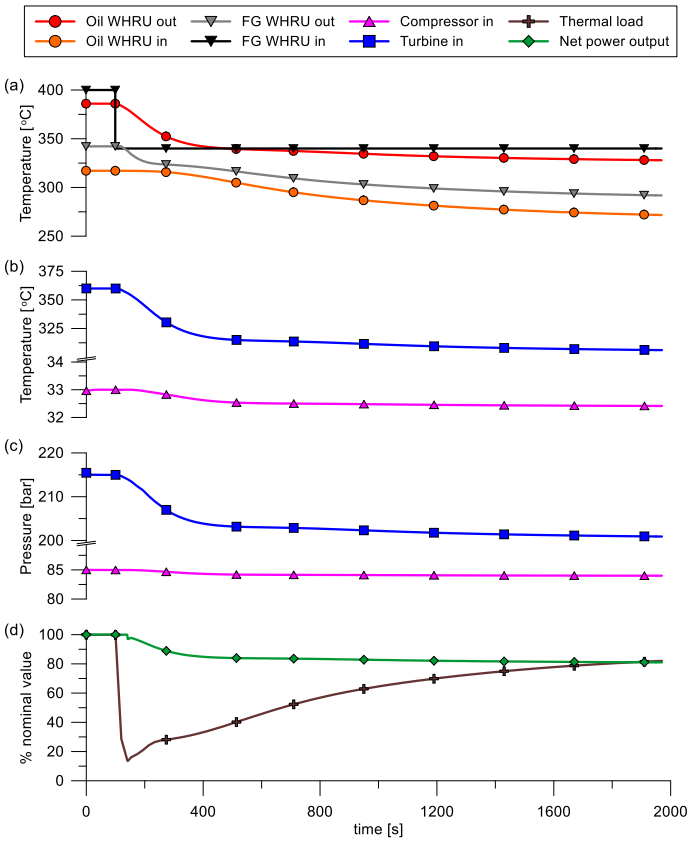

Figure 4: Open loop transient response to step change in exhaust gas temperature: (a) flue gas (FG) and oil temperatures at the inlet and outlet of the WHRU; (b) compressor and turbine inlet temperatures; (c) pressures, and (d) percentage variation of the cycle net power output and thermal load (waste heat recovered) in respect to the nominal value.

Figure shows the transient response of various parameters of the sCO_2 cycle to a step change in exhaust gas temperature from 400°C to 340°C (15% reduction), 100 seconds into operation at steady state conditions. This results in a drop of the temperature of the heat transfer oil at PHE inlet (WHRU outlet), from 385°C down to 325°C (Figure 4.a). Consequently, the oil temperature at the outlet of the PHE (WHRU inlet) also decreases from 317°C to 267°C. The decrease in temperature leads to an increase in the oil density and a 10% increase in the oil mass flow rate. The drop in the thermal oil temperature across the PHE leads to a 15% decrease in the CO_2 temperature at the turbine inlet (Figure 4.b) which in turn leads to variation in all other main cycle parameters such as the compressor inlet

DOI: 10.17185/duepublico/77321

temperature and pressure (Figure 4.b and 4.c respectively), the turbine inlet pressure (Figure 4.c) as well as the fluid thermodynamic conditions at the power turbine. In particular, while at the compressor inlet the temperature and pressure changes are 0.6°C and 1 bar respectively, the turbine inlet pressure shows a slightly higher change of 15 bar (Figure 4.c).

The new thermodynamic conditions reached by the cycle at steady state conditions after the step decrease of the flue gas temperature at the WHRU inlet lead to a 19% decrease in the net power output generated, Figure 4.d. This drop is caused mainly by a decrease in the power generated by the turbines, since the compressor power consumption stays approximately constant. In fact, higher variation of fluid thermodynamic conditions occurs at the inlet of the expander and power turbine, leading to a lower performance of these components. The thermal load available at the WHRU also decreases by 12% (Figure 4.d), meaning that the thermal efficiency of the cycle drops as well.

From a dynamic perspective, the turbine inlet temperature and pressure show a time constant of 313s (Figure 4.b and 4.c respectively). The other cycle parameters show similar transient behaviour. The large thermal inertia introduced by the metal mass of the heat exchangers and pipes as well as the thermal oil, is not sufficient to damp the temperature fluctuations of the flue gas. A 60°C temperature drop of the exhaust gas results in a temperature decrease rate of 10.8°C/min, which may exceed the thermal stress limits of the components. In such a case, controls should be implemented to reduce the rate of temperature reduction to protect the components from premature failure.

A similar trend can be noticed in the case of a step change in the exhaust gas mass flow rate (Figure 5). Similar to the case of step decrease in exhaust gas temperature, a 15% step reduction in exhaust gas mass flowrate was introduced 100s into operation at steady state conditions. However, in this case the magnitude of the variations is lower compared to the step change in exhaust gas temperature. Figure 5.a shows that the 15% step decrease in the mass flow rate of the exhaust gases leads to a reduced drop in the temperature of the thermal oil, and a reduction in the temperature of the sCO_2 at the turbine inlet, Figure 5.b.

Figure 5.c, shows that the step change in exhaust gas flowrate leads to a reduction in the pressure ratio across the sCO_2 cycle and approximately a 3% reduction in power generated compared to the 15% reduction in the case of the step change in exhaust gas temperature, Figure 4.d. These results demonstrate that the effect of reduction in the exhaust mass flowrate is partially compensated by increased temperature difference across the WHRU.

Table 5: Results of open loop transient response to a 15% step decrease in flue gas (FG) temperature while keeping the flue gas mass flow rate and the cooling conditions (air temperature and flow rate) constant. Cooling air temperature equal to 20°C and 297 kg/s respectively.

Parameters	Initial value	Final value	Time constant [s]
Flue gas mass flow rate	130 kg/s	130 kg/s	N/A
Flue gas inlet temperature	400°C	340°C	N/A
Thermal oil outlet temperature (from WHRU)	386°C	326°C	207
Thermal oil inlet temperature (to WHRU)	317°C	288°C	910
Thermal load	100% (9.10 MW)	88% (8.05 MW)	910
Turbine inlet temperature	360°C	304°C	213
Turbine inlet pressure	215.4 bar	200.8 bar	203
Compressor inlet temperature	33.0°C	32.4°C	313
Compressor inlet pressure	85.0 bar	84.0 bar	293
Net power output	100% (2.20 MW)	80% (1.77 MW)	203

Table 6: Results of open loop transient response to a 15% step decrease in flue gas (FG) mass flow rate while keeping the flue gas temperature and the cooling conditions (temperature and flow rate) constant. Cooling air temperature and mass flow rate equal to 20°C and 297 kg/s respectively.

Parameters	Initial value	Final value	Time constant [s]
Flue gas mass flow rate	130 kg/s	111 kg/s	N/A
Flue gas temperature	400°C	400°C	N/A
Thermal oil inlet temperature	386°C	379°C	490
Thermal oil outlet temperature	317°C	311°C	1140
Thermal load	100% (9.10 MW)	95% (8.62 MW)	1140
Turbine inlet temperature	360°C	354°C	350
Turbine inlet pressure	215.4 bar	211.2 bar	330
Compressor inlet temperature	33.1°C	33.0°C	545
Compressor inlet pressure	85.0 bar	84.9 bar	415
Net power output	100% (2.20 MW)	97% (2.14 MW)	330

DOI: 10.17185/duepublico/77321

Table 7: Results of open loop transient response to a 20% step decrease in cooling air mass flow rate while keeping the cooling air inlet temperature and the heating conditions constant. (Flue gas temperature and mass flow rate at 400°C and 130 kg/s respectively).

Parameters	Initial value	Final value	Time constant [s]
Air mass flow rate	297 kg/s	238 kg/s	N/A
Air inlet temperature	20°C	20°C	N/A
Air outlet temperature	42.9	46.9°C	89
Cooling load	100% (6.9 MW)	94% (6.4 MW)	89
Turbine inlet temperature	360°C	338°C	140
Turbine inlet pressure	215.4 bar	209.2 bar	94
Compressor inlet temperature	33.0°C	32.7°C	104
Compressor inlet pressure	85.0 bar	84.6 bar	90
Net power output	100% (2.20 MW)	93% (2.05 MW)	94

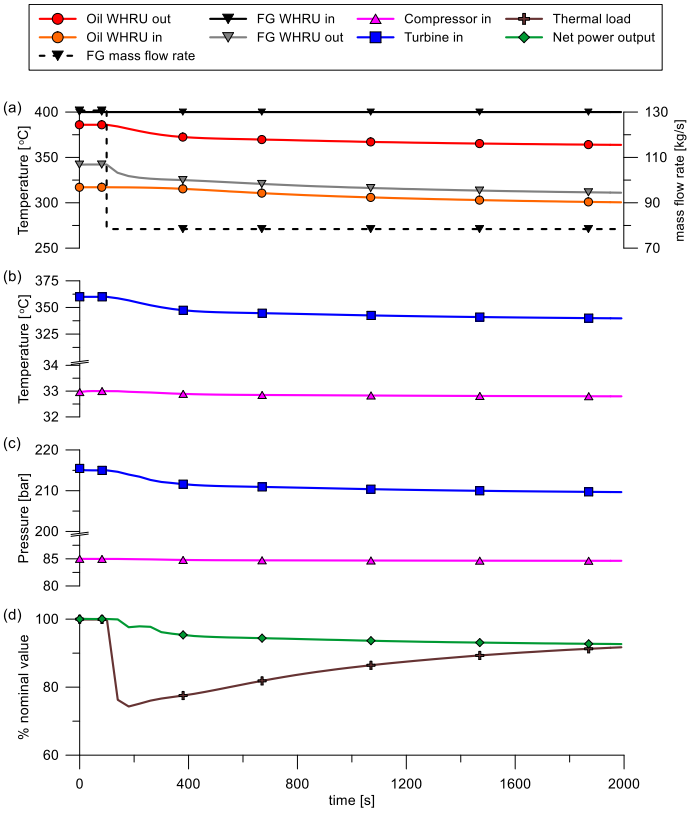

Figure 5: Open loop transient response to step change in exhaust gas mass flow rate: (a) flue gas (FG) and oil temperatures at the inlet and outlet of the WHRU: (b) compressor and turbine inlet temperatures and c) and pressures; (d) percentage variation of the cycle net power output and the waste thermal load recovered in respect to the nominal value.

Compared to the flue gas temperature step reduction case, the transient response of the cycle parameters is slower when a drop in the flue gas mass flow rate occurs. Figure 5 shows for instance that the time constant of the temperature and pressure at the turbine inlet is 350s and 330s respectively. For mass flow rate variations of the flue gas, the risk of component damage due to thermal stress is low as the rate of temperature decrease is only 2.8°C/min (Figure 5.b).

Since the changes in thermodynamic conditions of the cycle from the step change in exhaust mass flow rate investigated are quite small, the thermal load available when the new steady state is reached is only 5% lower than the initial steady state value (Figure 5.d).

Figure 6 shows the results for a step decrease in the air flow rate provided by the cooler. Such variation could be caused by a failure of one of the heat exchanger fans.

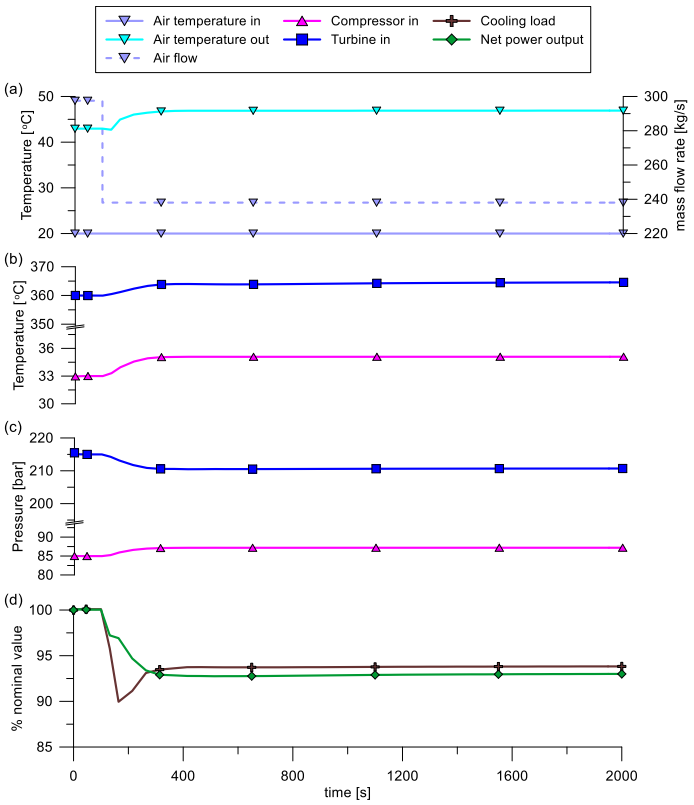

Figure 6: Open loop transient response to step change in air flow rate provided by the ACHE: (a) air mass flow rate and temperature at the inlet and outlet of the ACHE; (b), compressor and turbine inlet temperatures and (c) and pressures; (d) percentage variation of the cycle net power output and of cooling available at the ACHE with respect to the nominal value.

DOI: 10.17185/duepublico/77321

Figure 6.a shows the increase in the air temperature at the outlet of the ACHE following a 20% step decrease in the air mass flow rate provided by the fans. It can be seen that the cooling capacity available decreases by 8% (figure 6.d), and leads to a 2 ^{o}C increase in the compressor inlet temperature, which rises from 33°C to 35°C (Figure 6.b). As a consequence, the turbine inlet temperature increases as well, from 360°C to 365°C. At these conditions, the compressor operates at off-design, which leads to a reduction in the pressure ratio across the two turbines. This lower pressure ratio together with the reduced efficiency of the compressor itself cause a drop of 17% in the net power output generated by the system(Figure 6.d). These results show that the performance of the unit is very sensitive to variation of the cooling capacity of the heat rejection heat exchanger and this, if not controlled effectively, can have a negative impact on the operation of the component and other major components in the system.

Figure 6 also shows that the sCO_2 cycle transient response to the 20% step change in air mass flow rate has a time constant in the order of 100s which is much shorter compared to those of step changes in exhaust gas conditions. The lower time constant shows that an eventual control action on the cooler fans results in a prompt response of the temperature at the outlet of the cooler. For prompter control, cooler by-pass must be considered.

Dynamic response to actual variations in exhaust gas conditions and ambient air flowrate

One of the key contributions of this work is the study of the dynamic performance of sCO_2 WHP plant using actual real-time variations in exhaust gas and ambient air conditions. Simulations were performed to understand the dynamic behaviour of the sCO_2 cycle to actual fluctuations in the cement plant exhaust gas flow rate and temperature as well as changes in ambient air temperature over a 24-hour period. A sample data consisting of the exhaust gas and ambient air conditions on 17 July 2021 was used for the simulation (Figure 7). The variations in the exhaust gas flow rate is shown in **Error! Reference source not found.**.a. The maximum and minimum flow rate values were approximately 168 kg/s and 66 kg/s respectively. However, for most of the time, the exhaust gas flow rate remained relatively constant at 144 kg/s, except for some periods of large drop in flow rate. For instance, about 54% drop in flow rate, which lasted for about 20 minutes, occurred at 2:24 pm. The design operating point for the WHP plant was set close to the average value of the flow rate to cater for periods of dip in value. This would also ensure the availability of sufficient thermal energy in the exhaust gases for the heat transfer oil during periods of reduced exhaust gas temperature and high exhaust gas flow rate.

Variations in exhaust gas temperature are shown in **Error! Reference source not found.**.b and indicate a maximum value of 403°C and minimum value of 378°C. The exhaust gas temperature is seen to vary widely between the minimum and maximum value during the 24-hour
period. The design operating point value was chosen as 400°C to be near the maximum exhaust gas temperature and enable the WHP plant to be operated as efficiently as possible. The ambient air temperature variation for the 24-hour at the cement plant is shown in **Error! Reference source not found.**7.c. As expected, the ambient temperature started to increase at dawn and reached maximum value of 32°C at 3:25 pm before starting to decrease into the night time. This is in no way a depiction of typical variation in ambient air condition at the cement plant as the ambient condition could vary considerably depending on the time of the year. A look at data across the whole year indicates ambient temperatures as low as -13°C in the winter and reaching as high as 41°C in the summer.

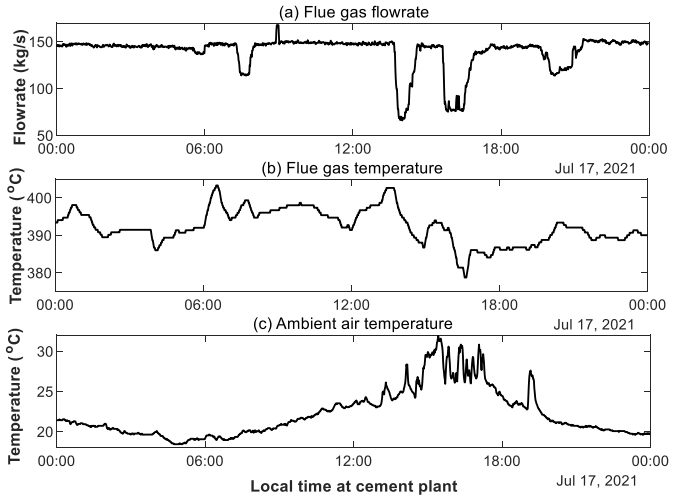

Figure 7: Actual real-time variations in exhaust gas conditions and ambient air temperature at the cement plant on 17th July, 2021

The dynamic response to combined variations in exhaust gas and ambient air conditions was simulated to show a realistic dynamic behaviour of the plant. Figure 8 shows the results of these simulations. In particular, Figures 8.a and 8.b show the variations of the turbine and compressor inlet temperatures respectively. Figure 8.c shows the variations in the duty of the main heat exchangers in the plant while Figures 8.d and 8.e show the performance of the sCO_2 unit in terms of net power output and efficiency.

The results show that from the parameters investigated, variations in ambient air temperature have the most significant impact on plant performance. The transients of the sCO_2 cycle variables look similar to the transients, of the ambient air temperature. This could be due to the fact that changes in ambient air temperature directly affect the compressor inlet temperature through the CO_2 gas cooler unlike the exhaust gas conditions which are damped by the intermediate oil loop.

The results also highlight the sensitivity of the sCO_2 cycle to changes in CO_2 properties close to the critical point at compressor inlet. Therefore, any control strategy for the sCO_2 cycle needs to consider the control of the gas cooler outlet (or compressor inlet) temperature or density [23] within the design operating value. This could be achieved through air recirculation and manipulation of air flow rate through the gas cooler. Control of the sCO_2 cycle for variations in exhaust gas conditions (within

DOI: 10.17185/duepublico/77321

allowable operation limit) might not be as imperative as gas cooler control. For instance, when exhaust gas flow rate or temperature drops, it may be appropriate not to take any control action as long as the cycle stays within the design operating envelope. Any attempt to control the sCO_2 cycle either through CO_2 bypass or reduction in CO_2 mass flow rate will lead to reduction in waste heat recovery capacity and may force the turbomachinery to operate further away from the design point. Exhaust gas data from the cement plant indicate that values are not expected to increase significantly above the design envelope and if this occurs it can be addressed effectively through oil by-pass control at the PHE.

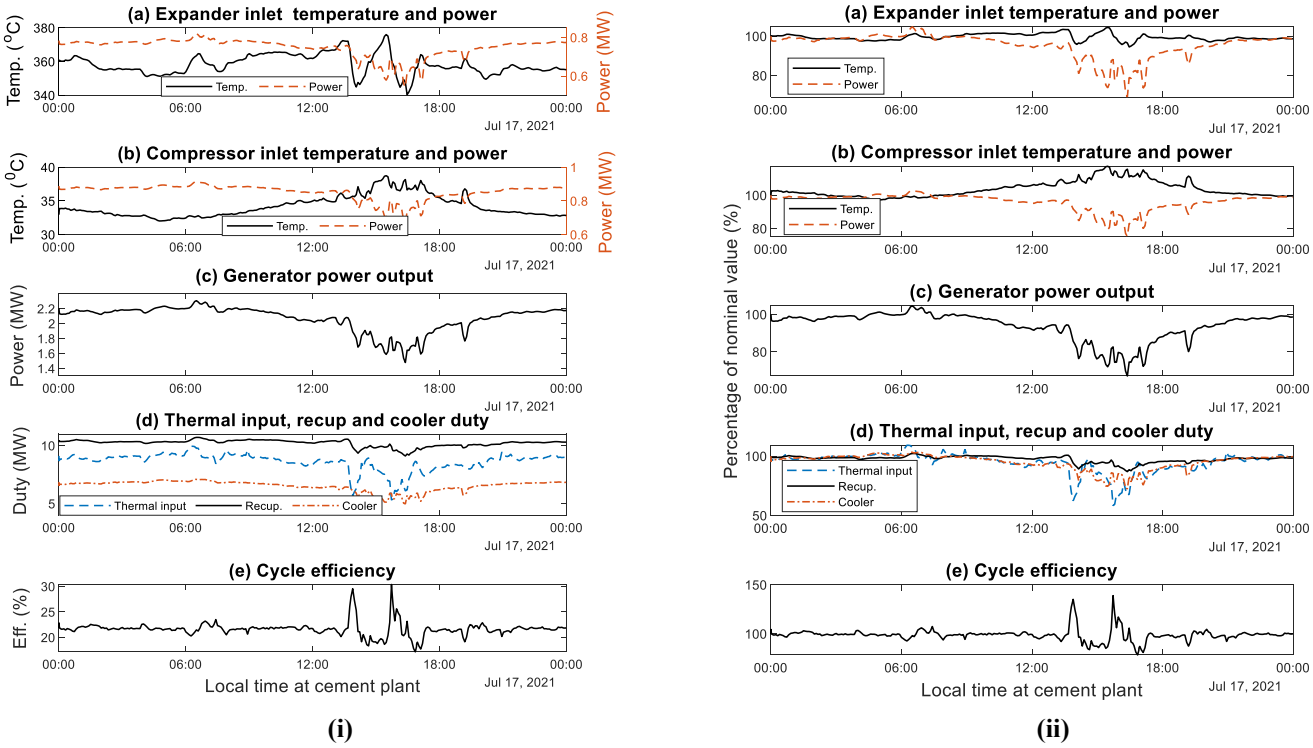

(i) (ii)

Figure 8: Dynamic response to combined actual real-time variations in exhaust gas conditions and ambient air temperature at the cement plant on 17th July, 2021: in absolute values (i) and in percentage variation from nominal conditions (ii)

Discussion on possible control strategies

One of the main advantages of adopting power units based on sCO2 technology is the potential flexibility of such systems in adapting quickly to large variations in operating conditions and being more efficient compared to conventional systems both at full and part load as well as during startups and shutdowns [24]. This is a desired feature for base load power systems, especially in a scenario characterized by a higher penetration of renewables and decentralized energy systems, but also for waste heat recovery applications.

Sudden and unforeseen variations in the waste heat source temperature or flow rate, may in fact require frequent shutdowns and startups of the power block, increasing plant idle times. This may lead to a decreased utilisation rate of the unit and prevent the maximization of economic benefits. Moreover, a reduced operating part-load range will increase further the need of shutting the system down in case of large variations in the waste heat source from nominal conditions.

Despite the potential of sCO2 power technology, limitations may arise during transients and at part-load conditions such as: compressor instabilities; turbine choking; CO_2 pressures and temperatures above design values; excessive shaft rotational speeds; and heat rejection requirements exceeding the capacity of the cooler [25]. In addition, the control systems should also be able to meet thermal load variations and ramp rates, keeping cycle efficiency at an optimal level and damping process disturbances such as small variations in heat input or heat rejection capacity particularly when direct heat rejection to air is employed [26].

To achieve these objectives among the main cycle variables to control are the compressor and turbine inlet conditions. The compressor inlet conditions are particularly important since, as showed in the previous sections, have a strong effect on system performance. With reference to the system analysed in this research, the control variables suitable to regulate the compressor inlet conditions are the regulation of the cooling load (air mass flow rate and cooler by-pass), mass flow rate recirculation (compressor by-pass), as well as shaft speed and inventory control.

If inventory control is not implemented due to its complexity, meaning that the fluid mass in the circuit is fixed, the isobaric regulation of the compressor temperature requires the simultaneous regulation of the turbine inlet temperature as well [27]. This can be done through by-passing the waste heat

DOI: 10.17185/duepublico/77321

recovery unit or controlling the mass flow rate of the intermediate heat transfer fluid (i.e. thermal oil). However, this control action can be actuated only in one direction (to decrease the turbine inlet temperature) since it is not usually possible to increase the thermal grade of the waste heat available.

The response to such changes, depend on the thermal inertia of the different components in the system as well as the ratio between the hot and cold volumes in the power block [28]. Reduced hot-and-cold volume ratios lead to reduced time constants and inertia while larger ones lead to slower dynamic response.

Other approaches are turbine flow bypass and throttling as well as the regulation of the shaft speed [29]. Even though such strategies typically lead to faster dynamic response, they also cause variations in CO_2 pressures in the circuit. Turbine by-pass and throttling flow control are usually employed in emergency scenarios and to adjust the power generated by the system to the load [29]. However, they could also be used to regulate the main compressor when it is driven by an expander.

The regulation of the shaft speed may also be used to control the compressor and turbine inlet conditions, but requires particular attention in the design of the compressor operating maps to avoid the occurrence of instabilities.

When inventory control is implemented, it is possible to regulate the density in the different parts of the system and therefore the conditions at the inlet of the turbomachines. Despite its slower response, it was found to be an efficient strategy to maximise the cycle efficiency at part-load conditions [25] but stability considerations due to the withdrawals/additions of CO_2 have been identified as a major issue to be addressed. Other key limiting factors in inventory control lie in the finite capacity of the storage tanks as well as the need of having ancillary control equipment which can substantially increase the cost of the power block. [30,31].

Figure 9 shows a possible arrangement of the different equipment required in the CO2OLHEAT demonstrator to realise the control strategies discussed in this section.

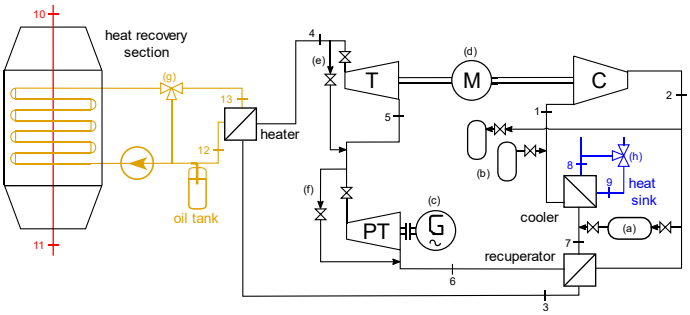

Figure 9: CO2OLHEAT sCO_2 available control variables: (a) compressor flow recirculation; (b), inventory control; (c) power turbine (PT) shaft speed; (d) TurboExpander (TE) shaft speed, (e) Expander (T) by-pass and throttling flow control (f) Power Turbine (PT) by-pass and throttling flow control (g) Waste Heat Recovery Unit (WHRU) by-pass; (h) Power Turbine (PT) by-pass and throttling flow control.

CONCLUSIONS

In this work a numerical model for a 2.0 MW sCO_2 power unit is presented. The model is suitable for dynamic simulation and control studies given the reduced computational effort required for each simulation.

The model has been used to investigate the system's transient response to variations in exhaust heat parameters and ambient temperature during a typical day at the a cement plant.

The main findings from the analysis show that variation of heat rejection to ambient air conditions have the strongest impact on system performance since they impact on the sCO_2 temperature at the compressor inlet. An increase of 8°C in the ambient temperature leads to a CO_2 temperature rise of 6°C at the compressor inlet. This suggests that control strategies must be designed to deal with such disturbances during operation, given that the system performance are sensitive to the compressor inlet temperature. When the compressor inlet temperature increases by 18%, the net power output of the system shows approximately a 20% decrease.

Small variations in exhaust gas parameters are cushioned by the thermal mass of components, particularly by the thermal oil in the indirect heat transfer loop.

In general, the results show that fast and accurate control of the CO_2 conditions at compressor inlet is key to ensuring reliable and efficient system performance. The system thermal inertia can filter small fluctuations in exhaust gas conditions reducing the impact on the turbine inlet temperature and control complexity.

NOMENCLATURE

Abbreviations

ACHE	Air-cooled heat exchanger
NIST	National Institute of Standards and Technology
PHE	Primary heat exchanger
sCO_2	supercritical carbon dioxide
WHP	Waste heat to power
WHR	Waste heat recovery
WHRU	Waste heat recovery unit

Symbols

A	Area (m^2)
D	Diameter (m)
f	Friction factor (-)
g	Acceleration due to gravity (m/s^2)
H	Liquid height or level (m)
h	Specific enthalpy (J/kg)
I	Inertia ($kg.m^2$)
L	Length (m)
M	Mass (kg)
$\dot{m}$	Mass flow rate (kg/s)
N	Rotational speed (rev/s)
P	Power (watt or J/s)
p	Pressure (Pa)
R	Gear ratio
T	Temperature (K)

DOI: 10.17185/duepublico/77321

t	Time (seconds)
U	Impeller tip speed (rad/sec)
u	Specific internal energy (J/kg)
v	Velocity (m/s)
Q	Heat transfer rate or duty (watt or J/s)
Δ	Increment or change
ρ	Density (kg/m^3)
φ	Heat flux (W/m^2)
ϕ	Flow coefficient
ω	Perimeter (m)

Subscripts

atm	Atmospheric
c	Cold stream
cc	Compressor
exp	Expander
HPC	High Pressure Compressor
h	Hydraulic or hot stream
in	Inlet
LPC	Low Pressure Compressor
m	Motor
out	Outlet
s	Surface
w	Metal wall

ACKNOWLEDGEMENTS

The CO2OLHEAT project has received funding from the European Union's Horizon 2020 research and innovation programme under grant agreement N° 101022831. The authors would like to acknowledge this funding as well as funding received from the Engineering and Physical Sciences Research Council (EPSRC) UK, for the SCOTWAHR project, grant reference EP/V001795/1. Exhaust gas data have been provided by CEMEX, a partner in CO2OLHEAT, whose contribution is gratefully acknowledged. Data related to the paper and other information relating to the paper can be obtained by contacting the corresponding author.

REFERENCES

[1] Cullen JM, Allwood JM. Theoretical efficiency limits for energy conversion devices. Energy 2010; 35:2059–69. https://doi.org/10.1016/J.ENERGY.2010.01.024.

[2] Forman C, Muritala IK, Pardemann R, Meyer B. Estimating the global waste heat potential. Renewable and Sustainable Energy Reviews 2016;57:1568–79. https://doi.org/10.1016/J.RSER.2015.12.192.

[3] Marchionni M, Bianchi G, Tassou SA. Review of supercritical carbon dioxide (sCO_2) technologies for high-grade waste heat to power conversion. SN Appl Sci 2020;2:1–13. https://doi.org/10.1007/s42452-020-2116-6.

[4] Crespi F, Gavagnin G, Sánchez D, Martínez G. Supercritical carbon dioxide cycles for power generation: A review. Appl Energy 2017.

[5] Kulhánek M, Dostál V. Supercritical Carbon Dioxide Cycles Thermodynamic Analysis and Comparison. Proceedings of $SCCO_2$ Power Cycle Symposium 2011:1–12.

[6] Marchionni M, Bianchi G, Tassou SA. Techno-economic assessment of Joule-Brayton cycle architectures for heat to power conversion from high-grade heat sources using CO_2 in the supercritical state. Energy 2018;148:1140–52. https://doi.org/10.1016/J.ENERGY.2018.02.005.

[7] Chai L, Tassou SA. Numerical study of the thermohydraulic performance of printed circuit heat exchangers for supercritical CO_2 Brayton cycle applications. Energy Procedia 2019; 161:480–8.https://doi.org/10.1016/j.egypro.2019.02.066.

[8] Marchionni M, Chai L, Bianchi G, Tassou SA. Numerical modelling and transient analysis of a printed circuit heat exchanger used as recuperator for supercritical CO2 heat to power conversion systems. Appl Therm Eng 2019;161:114190. https://doi.org/10.1016/j.applthermaleng.2019.114190.

[9] Baltadjiev ND, Lettieri C, Spakovszky ZS. An investigation of real gas effects in supercritical CO2 centrifugal compressors. Journal of Turbomachinery. 2015 Sep 1;137(9):091003. https://doi.org/10.1115/1.4029616

[10] Fuller, Robert L, Eisemann K. Centrifugal Compressor Off-design performance for supercritical CO2. Supercritical CO2 Power Cycle Symposium, Boulder, Colorado: 2011, p. 12.

[11] Thatte A, Loghin A, Shin Y, Ananthasayanam B. Performance and Life Characteristics of Hybrid Gas Bearing in a 10 MW Supercritical CO_2 Turbine. Volume 9: Oil and Gas Applications; Supercritical CO_2 Power Cycles; Wind Energy, ASME; 2016, p. V009T36A018. https://doi.org/10.1115/GT2016-57695.

[12] Alfani D, Astolfi M, Binotti M, Silva P. Part load strategy definition and annual simulation for small size sCO_2 based pulverized coal power plant. Proceedings of the ASME Turbo Expo, vol. 11, American Society of Mechanical Engineers (ASME); 2020. https://doi.org/10.1115/GT2020-15541.

[13] Marchionni M, Saravi SS, Bianchi G, Tassou SA. Modelling and performance analysis of a supercritical CO_2 system for high temperature industrial heat to power conversion at off-design conditions. 3rd European sCO_2 conference, 2019. https://doi.org/10.17185/duepublico/48908.

[14] Supercritical CO2 power cycles demonstration in Operational environment Locally valorising industrial Waste Heat. CO2OLHEAT Project H2020. European Commission. https://cordis.europa.eu/project/id/101022831 (accessed October 26, 2022).

[15] Ozana S and Macháček Z. Implementation of the mathematical model of a generating block in matlab and simulink using s-functions. The Second International Conference on Computerand Electrical Engineering ICCEE.Session 8. p. 431-435.2009.

[16] Lemmon EW, Bell IH, Huber ML, McLinden MO. NIST Standard Reference Database 23: Reference Fluid Thermodynamic and Transport Properties (REFPROP), Version 10.0; National Institute of Standards and Technology, Standard Reference Data Program:Gaithersburg, MA, USA, 2018.

DOI: 10.17185/duepublico/77321

[17] Franke R, Casella F, Sielemann M, Proelss K, Otter M. Standardization of thermo-fluid modelling in Modelica. Fluid. In Proceedings of the 7th International Modelica Conference 2009 (pp. 122-131). Linköping University Electronic Press.

[18] Pham HS, Alpy N, Ferrasse, JH, Boutin O, Tothill M, Quenaut J, Gastaldi O, Cadiou T, Saez M. An approach for establishing the performance maps of the sc-CO2 compressor: Development and qualification by means of CFD simulations. International Journal of Heat and Fluid Flow 2016, 61, pp.379-394. https://doi.org/10.1016/j.ijheatfluidflow.2016.05.017

[19] Lambruschini F, Liese E, Zitney SE, Traverso A. Dynamic model of a 10 MW supercritical CO2 recompression Brayton cycle. InTurbo Expo: Power for Land, Sea, and Air 2016 Jun 13 (Vol. 49873, p. V009T36A004). American Society of Mechanical Engineers. https://doi.org/10.1115/GT2016-56459

[20] Gong Y, Carstens NA, Driscoll MJ, Matthews I. Analysis of radial compressor options for supercritical CO2 power conversion cycles. Massachusetts (USA): Center for Advanced Nuclear Energy Systems 2006.

[21] Zhang Y, Li H, Li K, Yang Y, Zhou Y, Zhang X, Xu R, Zhuge W, Lei X, Dan G. Dynamic characteristics and control strategies of the supercritical CO2 Brayton cycle tailored for the new generation concentrating solar power. Applied Energy 2022; 328, p.120190. https://doi.org/10.1016/j.apenergy.2022.120190

[22] Olumayegun O, Wang M. Dynamic modelling and control of supercritical CO_2 power cycle using waste heat from industrial processes. Fuel 2019; 249:89–102. https://doi.org/10.1016/J.FUEL.2019.03.078.

[23] Casella F, Mangola G, Alfani D. Density-Based Control of Air Coolers in Supercritical CO2 Power Cycles. IFAC-Papers OnLine, 53 (2), 2020:12554-12559. https://doi.org/10.1016/j.ifacol.2020.12.1810

[24] Cagnac A, Mecheri M, Bedogni S. Configuration of a flexible and efficient sCO2 cycle for fossil power plant. 3rd European Supercritical CO2 Conference, 19-20 September, Paris, France, 2019, https://dx.doi.org/10.17185/duepublico/48907.

[25] Trinh TQ. Dynamic Response of the Supercritical CO2 Brayton Recompression Cycle to Various System Transients (Ph.D. thesis), Massachusetts Institute of Technology, 2009.

[26] P. Mahapatra, S.E. Zitney, J. Albright, E.A. Liese, Advanced regulatory control of a 10 MWe supercritical CO_2 recompression Brayton cycle towards improving power ramp rates, in: The 6th International Symposium on Supercritical CO_2 Power Cycles, 27-29 March, Pittsburgh Pennsylvania, 2018.

[27] N. Carstens, Dynamic Response and Safety Implications for Supercritical CO_2 Brayton Cycles Coupled to Gen-IV Reactors (Ph.D. thesis), Massachusetts Institute of Technology, 2007.

[28] Hacks AJ, Schuster S, Brillert D. Impact of volumetric system design on compressor inlet conditions in supercritical CO2 cycles. Journal of the Global Power and Propulsion Society. 2021;5:104-110. https://dx.doi:10.33737/jgpps/140118.

[29] J. Kwon, J.I. Lee, Development of accelerated PCHE off-design performance model for optimizing power system control strategies in s-CO_2 system, in: The 6th International Symposium on Supercritical CO_2 Power Cycles, 27-29 March, Pittsburgh Pennsylvania, 2018.

[30] Marchionni M, Usman M, Chai L, Tassou SA. Inventory control assessment for small scale sCO2 heat to power conversion systems. Energy. 2022 Dec 26:126537. https://doi.org/10.1016/j.energy.2022.126537

[31] B.S. Oh, J.I. Lee, Study of autonomous control system for s-CO_2 power cycle, in: 3rd European Supercritical CO2 Conference, 19-20 September, Paris, France, 2019, pp. 345–352, http://dx.doi.org/10.17185/duepublico/48913, 145.

 DOI: 10.17185/duepublico/77321

DOI: 10.17185/duepublico/77321
URN: urn:nbn:de:hbz:465-20230427-144432-2